Applied Vegetation Science 13: 72–85, 2010
DOI: 10.1111/j.1654-109X.2009.01051.x

Spatial variability of above-ground net primary production in Uruguayan grasslands: a remote sensing approach

S. Baeza, F. Lezama, G. Piñeiro, A. Altesor & J. M. Paruelo

Abstract

Question: How does above-ground net primary production (ANPP) differ (estimated from remotely sensed data) among vegetation units in sub-humid temperate grasslands?

Location: Centre-north Uruguay.

Methods: A vegetation map of the study area was generated from LANDSAT imagery and the landscape configuration described. The functional heterogeneity of mapping units was analysed in terms of the fraction of photosynthetically active radiation absorbed by green vegetation (fPAR), calculated from the normalized difference vegetation index (NDVI) images provided by the moderate resolution imaging spectroradiometer (MODIS) sensor. Finally, the ANPP of each grassland class was estimated using NDVI and climatic data.

Results: Supervised classification presented a good overall accuracy and moderate to good average accuracy for grassland classes. Meso-xerophytic grasslands occupied 45% of the area, Meso-hydrophytic grasslands 43% and Lithophytic steppes 6%. The landscape was shaped by a matrix of large, unfragmented patches of Meso-xerophytic and Meso-hydrophytic grasslands. The region presented the lowest anthropic fragmentation degree reported for the Rio de la Plata grasslands. All grassland units showed bimodal annual fPAR seasonality, with spring and autumn peaks. Meso-hydrophytic grasslands showed a radiation interception 10% higher than the other units. On an annual basis, Meso-hydrophytic grasslands produced 3800 kg dry matter (DM) ha^{-1} yr^{-1} and Meso-xerophytic grasslands and Lithophytic steppes around 3400 $kg \cdot DM \cdot ha^{-1} \cdot yr^{-1}$. Meso-xerophytic grasslands had the largest spatial variation during most of the year. The ANPP temporal variation was higher than the fPAR variability.

Conclusions: Our results provide valuable information for grazing management (identifying spatial and temporal variations of ANPP) and grassland conservation (identifying the spatial distribution of vegetation units).

Keywords: Land-cover classification; Native grasslands; Normalized difference vegetation index (NDVI); Radiation-use efficiency; Río de la Plata grasslands.

Nomenclature: Zuloaga et al. (1994), Zuloaga & Morrone (1996a,b).

Abbreviations: ANPP = Above-ground net primary production; fPAR = Fraction of photosynthetically active radiation absorbed by green vegetation; NDVI = Normalized difference vegetation index; APAR = Photosynthetically active vegetation absorbed by the canopy.

Baeza, S. (corresponding author, sbaeza@fcien.edu.uy) & **Altesor A. (**aaltesor@fcien.edu.uy**)**: Sección Ecología Terrestre, Departamento de Ecología, Facultad de Ciencias, Universidad de la República, Iguá 4225, Montevideo, Uruguay.

Lezama F. (flezama@tyt.inia.org.uy): Instituto Nacional de Investigación Agropecuaria, Ruta 8 km282, Treinta y Tres CP 33000, Uruguay.

Piñeiro G. (pineiro@ifeva.edu.ar): Laboratorio de Análisis Regional y Teledetección, IFEVA, Facultad de Agronomía, Universidad de Buenos Aires/CONICET, Av. San Martin 4453, C1417DSE, Buenos Aires, Argentina.

Paruelo J.M. (paruelo@agro.uba.ar): Sección Ecología Terrestre, Departamento de Ecología, Facultad de Ciencias, Universidad de la República, Iguá 4225, Montevideo, Uruguay; Laboratorio de Análisis Regional y Teledetección, IFEVA, Facultad de Agronomía, Universidad de Buenos Aires/CONICET, Av. San Martin 4453, C1417DSE, Buenos Aires, Argentina.

Introduction

The description of the spatial and temporal variation of vegetation variables is a critical step in defining management actions in rangelands. Such characterization can be based either on structural or functional attributes. Structural approaches focus on floristic or physiognomic descriptions of communities or vegetation types. Functional approaches can be based on the relative abundance of plant functional types (Lavorel et al. 1997), and on the seasonal variation of the exchange of matter and energy between the biota and the environment (Paruelo et al. 2001). Above-ground net primary

production (ANPP) is an integrative descriptor of ecosystem functioning and it determines the total amount of available energy for upper trophic levels (McNaughton et al. 1989). For rangelands, ANPP is the main control of stock density (Oesterheld et al. 1998). There are many methodological alternatives for estimating ANPP, including biomass harvesting, empirical models relating ANPP and precipitation or remotely sensed data (Sala & Austin 2000).

Many attempts have been made to characterize land-cover patterns over extensive areas (thousands of square kilometres) using high-resolution satellite images (i.e. Brown de Colstoun et al. 2003; Guershman et al. 2003). These attempts were based on the differential spectral response of the distinct land cover types. Multitemporal data allows capture of a spectral signal related with phenological differences, increasing the ability to discriminate among land-cover units (Guershman et al. 2003).

Spectral indices and biophysical variables derived from remotely sensed data have been extensively used to quantify ecosystem functioning attributes such as primary production (Prince 1991), or evapotranspiration (Jackson et al. 1983). Most of these attempts have been based on the analysis of the seasonal variation of the normalized difference vegetation index (NDVI), a spectral index calculated from the reflectance in the red (R) and infrared (IR) portions of the electromagnetic spectrum [$NDVI = (IR - R)/(IR + R)$]. This index shows a positive and linear relationship with the fraction of photosynthetically active radiation absorbed by green vegetation (fPAR) and hence with primary production (Prince 1991; Di Bella et al. 2004; Piñeiro et al. 2006a). Monteith's model (1972) provides the conceptual link between fPAR (estimated from the NDVI) and primary production: ANPP is equivalent to the total amount of photosynthetically active vegetation absorbed by the canopy (APAR) multiplied by a radiation-use efficiency coefficient (see below). The use of Monteith's model increases significantly the correspondence between field and remotely sensed estimates of ANPP (Piñeiro et al. 2006a).

The Río de la Plata grasslands are one of largest areas of natural temperate sub-humid grasslands in the world (Soriano 1991; Paruelo et al. 2007). They occupy more than 70×10^6 ha in southern South America, including the Pampas in Argentina and the Campos in Uruguay and southern Brazil. An important portion of this region has been or is being modified by the expansion of agriculture and afforestation (Jobbágy et al. 2006; Paruelo et al. 2006). However, large areas are still dominated by natural (native) or semi-natural grasslands, grazed by cattle and sheep (Paruelo et al. 2007). Land use/land cover descriptions are scarce in the region (Paruelo et al. 2004a; Baldi et al. 2006; Baldi & Paruelo 2008), particularly those describing the floristic and physiognomic heterogeneity of rangelands. The characterization of structural (i.e. plant communities or physiognomic types) and functional (i.e. ANPP gradients) variation is a key step in designing sustainable rangeland management schemes or conservation plans. In Uruguay, livestock production is based mainly on extensive systems where animals graze large paddocks all year-round. Supplementation or more intensive grazing systems (i.e. rotational management) are not common. Traditional extensive management is characterized by the low production efficiency and it has been identified as a driver of grassland degradation (e.g. the reduction of the relative cover of plant species highly preferred by livestock) (Rodríguez et al. 2003). The lack of knowledge of the spatial distribution of grassland types (plant communities) and the interannual and seasonal variability of their productivity restrict, among other factors, the development of sustainable grazing management (Golluscio et al. 1998).

In this article we combined remote sensing data and a previous published phytosociological description of grassland communities (Lezama et al. 2006) to characterize the structure and functioning of the most extensive areas of natural grasslands in South America. Specifically, our goals were: (1) to map the main vegetation units defined by Lezama et al, 2006 for the Basaltic region in the centre-north portion of Uruguay; (2) to describe the degree of grassland fragmentation of the study area; (3) to characterize the functional heterogeneity of the mapped units in terms of fPAR, as derived from spectral indices; and (4) to estimate ANPP for each grassland class using NDVI and climatic data. Finally, we discuss how to integrate this information to devise management actions.

Materials and Methods

Study area

The study area is located in centre-north of Uruguay, on a geomorphological unit based on Basaltic rocks (Panario 1988) (31°35′S, 56°12′W and 32°12′S, 57°20′W). The analysis was restricted to two cartographic soil units: "Cuchilla de Haedo – Paso de los Toros" and "Queguay Chico" (Fig. 1). These soil units cover 1.5 million hectares with high percentages of natural grassland. The dominant soils in the study area are Hapludols and Udorthents associated with rock outcrops (Altamirano et al. 1976).

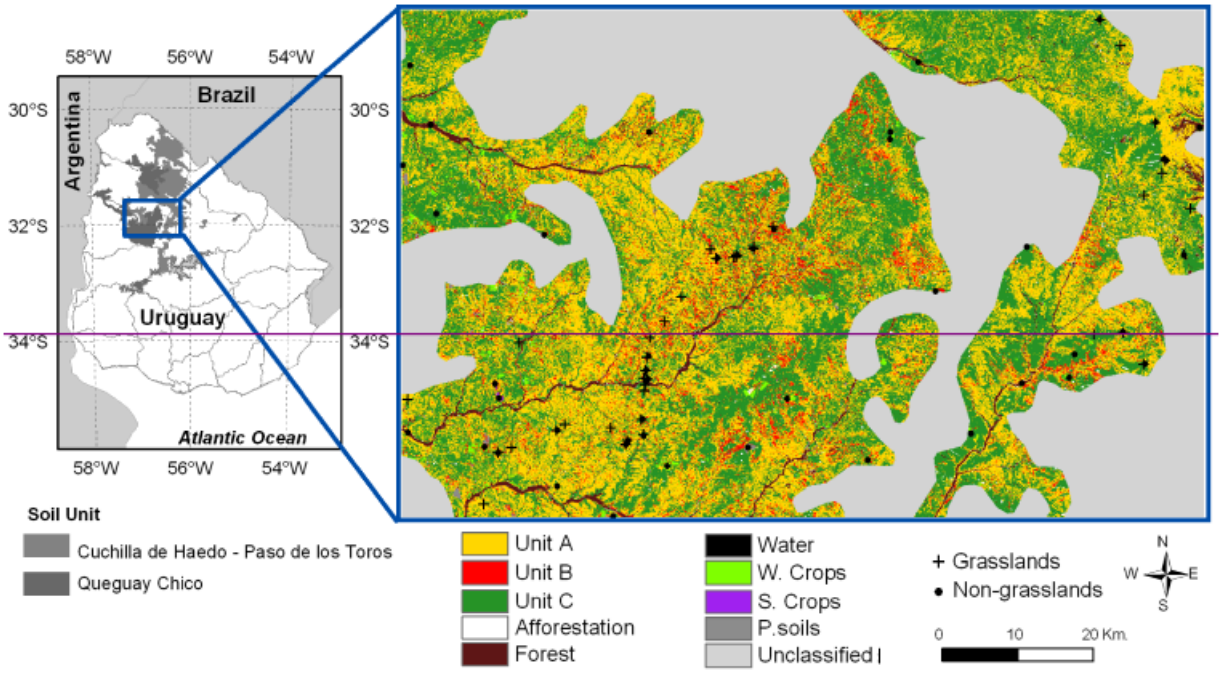

Fig. 1. Study area in centre-north Uruguay. Grey-tone areas correspond to the soil units analyzed. The rectangle shows the vegetation map of the study area derived from Landsat TM images. Unit A: Meso-xerophytic grasslands; Unit B: Lithophytic steppes; Unit C: Meso-hydrophytic grasslands; W. Crops: winter crops; S. Crops: summer crops; P. soils: Plowed soils in both dates of images acquisition. The location of the polygons used for training and evaluation process are showed with crosses (grassland releves) and dots (non-grassland areas).

The climate of the study areas is temperate to subtropical with a mean annual temperature of 18°C and mean annual precipitation around 1300 mm. (Dirección Nacional de Meteorología 2005).

Grassland heterogeneity of the region has been described using a phytosociological approach (Lezama et al. 2006). Based on vegetation and environmental variables recorded in 45 homogeneous stands, and from the classification of the species by stand matrix, Lezama et al. (2006) defined six communities grouped in three main vegetation units. The main units were named: Meso-xerophytic grasslands, Lithophytic steppes and Meso-hydrophytic grasslands (detailed description in App. 1). Ordination analysis showed that floristic variability was mainly associated with a gradient of water availability defined by soil depth, texture, slope and slope form (Lezama et al. 2006).

Spatial distribution of grassland units

Supervised classifications were performed on Landsat TM imagery (spatial resolution 30 m×30 m) to map the vegetation units described by Lezama et al. (2006). We used two images (Path, 224/Row, 082), corresponding to spring (30 September 1999) and early summer (28 December 2000), to capture phenological differences among units. Both images were radiometric and atmospherically corrected to make the spectral information comparable both in time and space (Chuvieco 2002). We calculated top-of-atmosphere reflectance values for each image using the headers' information. Atmospheric corrections were performed using the "dark object subtraction" method. This method estimates the relative atmosphere contribution in the total radiance received by the sensor from patches that should present null reflectance (shadow zones, water, etc.) and includes multiplicative corrections for the effect of atmospheric transmittance (Chavez 1996). The Sep image was georeferenced to Gauss-Krugger projection (Transverse Mercator; Ellipsoid: Hayford, international 1924; Datum: Yacaré) and the Dec image was co-registered to the first one. We generated a multitemporal image with 12 bands (six reflective bands for each date) to capture spectral differences in vegetation cover. The analyses were performed on a subset of the original images corresponding to the two soil units studied.

Nine land-cover classes were defined: afforestation, native forest, water bodies, winter crops,

summer crops, ploughed soils in both dates of image acquisition and three grassland types based on the units defined in the phytosociological analysis (Meso-xerophytic grasslands, Lithophytic steppes and Meso-hydrophytic grasslands). The training polygons for the first six classes were defined by photointerpretation of false-colour Landsat images (bands 4, 3 and 2). We identified 25 training polygons for the non-grassland classes. These classes presented a clear contrast with the grasslands units and its identification was simple. For the grassland units, 25 homogeneous vegetation stands sampled in Lezama's et al. (2006) phytosociological study were used as training polygons in the classification processes. The spectral information of six bands of each image and maximum likelihood decision rule were used to classify all the pixels of the study area (Lillesand & Kiefer 1994). The remaining 20 of Lezama's et al. (2006) vegetation stands and 25 polygons of the non-grassland classes were used the to evaluate the accuracy of the classification process. To evaluate the classification we calculated the Kappa coefficient and the overall accuracy from a contingency matrix based on polygons not used in the classification processes (Congalton 1991).

The degree of landscape fragmentation was analysed calculating the mean patch size (MPS) and the effective mesh size (EMS) indexes (Riitters et al. 1995). The EMS simultaneously takes into account the patch size and the level of dissection and it is not sensitive to the inclusion/omission of small patches; the greater the EMS, the lower is the fragmentation level (Jaeger 2000). We removed the "salt and pepper" appearance of supervised classification by applying a moving window majority filter (5×5 pixels). We grouped the grassland units (Meso-xerophytic grasslands, Lithophytic steppes and Meso-hydrophytic grasslands) and the ploughed soils, summer and winter crops, into a "grassland" and a "crop" class respectively. The remaining map was converted from raster to vector format in order to calculate MPS and EMS.

Vegetation functioning

We used NDVI images from the MODIS sensor (Moderate Resolution Imaging Spectroradiometer) onboard the EOS Terra satellite to characterize a key functioning attribute: the seasonality of light interception. The "MODIS Land Science Team" (http://modis-land.gsfc.nasa.gov/) produces an NDVI composite image every 16 days with a spatial resolution of 250 m×250 m. We used a NDVI time series corresponding to the period 2000-2004 (112 images). The MODIS images were projected to the same system used for Landsat images. Each NDVI image was filtered using its associated "per pixel" quality image (Roy et al. 2002) and only those pixels with acceptable or superior quality were analysed.

The supervised classification was intersected with a squared cell grid of 250 m×250 m where each cell corresponded to a MODIS pixel (Fig. 2). For each cell we identified the majority class (mode) on the supervised classification and its proportion within the cell. Only those cells with more than 75% of a single class were considered. The NDVI time series (112 values) was extracted for each cell. The image analyses and GIS operations were carried out with ERDAS 8.7 (Leyca Geosystems, Atlanta, GA, US) and ARCMAP-ARCGIS 8.3 (ESRI, Redlands, CA, US).

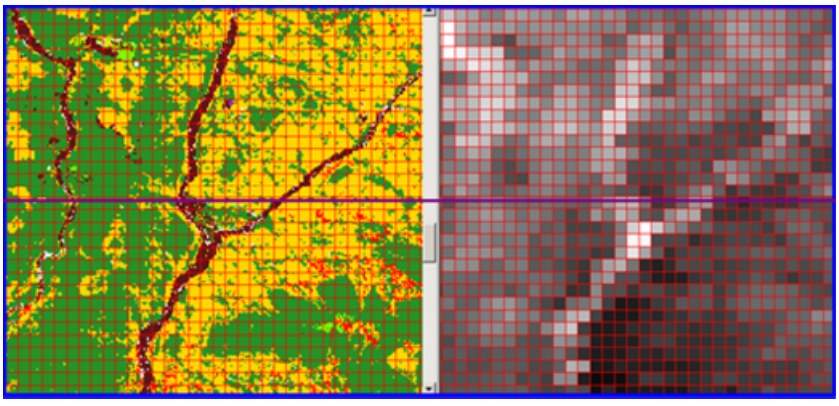

Fig. 2. Left, supervised classification of Landsat images. Right, the same portion of territory in a NDVI MODIS image. In Red, grid built from MODIS pixels. For each cell the majority class and the percentage of this class were extracted. Only those pixels with a percentage of a single class higher than 75% were considered in the functional analysis.

The NDVI values were transformed into fPAR using linear interpolation (Ruimy et al. 1994). The maximum NDVI was fixed as the 98th percentile of the time series (NDVI = 0.83), setting to 95% of fPAR interception (assuming saturation at high leaf area index values). The minimum NDVI was fixed as the 5th percentile of bare soil areas (NDVI = 0.215), setting to fPAR = 0. We obtained the following equation:

$$\mathrm{FPAR} = \mathrm{MIN}((-0.3321 + 1.5445 \times \mathrm{IVN});\ 0.95) \quad (1)$$

fPAR data derived from NDVI were used to estimate ANPP ($g \cdot DM \cdot m^{-2} \cdot d^{-1}$) using Monteith's (1972) model:

$$\mathrm{ANPP} = \mathrm{APAR} \times \varepsilon a = \mathrm{PAR} \times \mathrm{fPAR} \times \varepsilon a \quad (2)$$

where APAR is the total amount of photosynthetically active radiation absorbed by green vegetation ($MJ \cdot m^{-2} \cdot day^{-1}$), PAR is the incident photosynthetically active radiation ($MJ \cdot m^{-2} \cdot day^{-1}$), fPAR is the fraction of that radiation intercepted by green vegetation and εa the energy conversion coefficient of absorbed radiation into above-ground biomass ($g\,MJ^{-1}$). The PAR data were obtained from the BIOME BGC project (http://www.ntsg.umt.edu/cgi-bin/show_good_ncdc_stations.pl) and they corresponded to the nearest meteorological station (Salto: 31°24′S,57°58′W). We calculated average PAR values with the daily values for the 16-day intervals corresponding to the same dates of NDVI MODIS composites. The fPAR values were calculated from the NDVI MODIS images as described above. To estimate εa we followed the approach presented by Piñeiro et al. (2006a) and Piñeiro et al. (2004) where seasonal values of εa are calculated from an empirical relationship with climatic variables:

$$\varepsilon a = 0.36206 + \mathrm{pEf} \times 0.00214 - t\mathrm{max} \times 0.01141 \quad (3)$$

where pEF is the effective precipitation accumulated over the period of ANPP measurement and t_{max} is the average maximum temperature for the same period. Effective precipitation is the fraction of water effectively available for plants; it is calculated as a daily water balance based on precipitation, potential evapotranspiration and water holding capacity (Piñeiro et al. 2006b). Water-holding capacity was computed using pedotransfer functions based on texture data (Rawls 1983), and used to estimate runoff, a critical process needed to properly simulate water dynamics in landscapes with shallow soils. We used climatic data from the INIA Salto meteorological station (http://www.inia.org.uy/disciplinas/agroclima/banco_met). Equation 3 was specifically calibrated from local data included in the study area (Piñeiro et al. 2004). The ANPP was calculated for every grassland class and for 16-day intervals. Annual ANPP was calculated averaging the values of the 23 dates of the five growing season (July-June).

Monthly fPAR and ANPP values from each grassland class were averaged over the 5-year period and compared using repeated measures ANOVA. Vegetation unit was used as the independent variable and months of the average year were used as the repeated factor. We used a *post hoc* comparison Tukey HSD test (Zar 1996) to evaluate differences among pairs of classes. Statistical analyses were performed with STATISTICA 6.0. (Statsoft, Inc. Tulsa, OK, US).The spatial (among pixels pertaining to the same vegetation unit) and temporal (among years) variability of monthly APAR, fPAR and ANPP values was evaluated from the coefficient of variation.

Results

Spatial distribution of grassland units

The supervised classification of Landsat images showed that more than 90% of the study area is occupied by natural grasslands (Fig. 1). Of the 440 000 classified hectares, approximately 45% corresponded to Meso-xerophytic grasslands, 43% to Meso-hydrophytic grasslands, 6% to Lithophytic steppes, 3% to forest, 2% to winter crops and 1% to afforestation. The classes water, ploughed soils and summer crops were marginal and in total they covered only 0.5% of the classified area (Fig. 1). The contingency matrix showed an overall accuracy of 91.5%, and a value of kappa coefficient of 0.9. This high overall accuracy could be an artefact of the distribution of control pixels between the different classes because grassland classes represent only 32% of control pixels and 94% of the study area. The average accuracy for grassland classes was 76.8% (Table 1), a good result given the relative homogeneous physiognomy of these land-covers.

The landscape was conformed by a matrix of grasslands. On average, a patch of grassland covered 1962 ha, while native forest occupied 9.5 ha. The more modified land-covers (crops and afforestations) had, on average, patches smaller than 3.2 ha (Fig 3a). The natural land-covers (grasslands and native forests) are much less fragmented (high EMS) than implanted forests and crop areas (Fig. 3b).

Table 1. Contingency matrix among the classification results and field data expressed by (1) percentage and (2) pixel count. Percentages of correctly classified pixels are shown in bold type. Unit A = Meso-xerophytic grasslands; Unit B = Lithophytic steppes; Unit C = Meso-hydrophytic grasslands; W. Crops = winter crops; S. Crops = summer crops; Affor. = afforestation; P. soils = ploughed soils in both dates of images acquisition.

(1) Class	Land truth								
	Unit A	W. crops	S. crops	Water	Unit B	Unit C	Affor	Forest	P. soils
Classification									
1									
Unit A	**78.5**	0.0	0.0	0.0	25.6	17.7	1.7	0.1	0.0
W. Crops	0.0	**99.4**	0.0	0.0	0.0	0.0	0.9	0.1	0.0
S. Crops	0.0	0.0	**54.6**	0.0	0.0	0.0	0.0	0.0	0.0
Water	0.0	0.0	0.0	**100.0**	0.0	0.0	0.0	0.0	0.0
Unit B	4.0	0.0	0.0	0.0	**73.8**	0.7	0.0	0.0	0.0
Unit C	17.5	0.3	4.6	0.0	0.6	**78.2**	0.0	0.0	0.0
Affor	0.0	0.0	9.1	0.0	0.0	0.7	**85.3**	0.2	0.0
Forest	0.0	0.1	31.8	0.0	0.0	2.8	12.1	**99.5**	0.0
P. soils	0.0	0.1	0.0	0.0	0.0	0.0	0.0	0.0	**100.0**
Total	100	100	100	100	100	100	100	100	100
2									
Unit A	**274**	0	0	0	43	81	2	1	0
W. Crops	0	**687**	0	0	0	0	1	1	0
S. Crops	0	0	**12**	0	0	0	0	0	0
Water	0	0	0	**162**	0	0	0	0	0
Unit B	14	0	0	0	**124**	3	0	0	0
Unit C	61	2	1	0	1	**359**	0	0	0
Affor	0	0	2	0	0	3	**99**	2	0
Forest	0	1	7	0	0	13	14	**828**	0
P. soils	0	1	0	0	0	0	0	0	**210**
Total	349	691	22	162	168	459	116	832	210

Vegetation functioning

More than 34 000 "pure" cells (i.e. with more than 75% of the Landsat pixels belonging to a particular class within the cell) were identified by superimposing the square cell grid of 250 m × 250 m over the supervised classification (Fig. 2). All the grassland classes analysed showed a bimodal annual variation of fPAR, with a clearly defined spring peak (maximum values in Oct), a decrease in late spring-early summer and a gradual increase along the summer with maximum values in autumn (Fig. 4j). Despite some variations, this bimodal pattern was evident throughout all the growing season analysed (Fig. 4i). The highest fPAR values occurred in March 2003, on Meso-hydrophytic grasslands, when the vegetation absorbed 85% of the available photosynthetically active radiation (Fig. 4i). The lowest fPAR (39%) was observed in Mar 2004 on Lithophytic steppes (Fig. 4i). The Meso-hydrophytic grasslands had the highest values of fPAR, with a curve clearly different from the other two grassland classes (Fig. 4i,j). The Meso-xerophytic grasslands had higher average fPAR values than the Lithophytic steppes from October to March and were lower the rest of the year. The maximum average values of fPAR for all the classes occurred in autumn (May), whereas the minimum values occurred in summer (December) for the xerophytes classes (Meso-xerophytic grasslands and Lithophytic steppes) and in winter for the Meso-hydrophytic grasslands (Fig. 4j).

The 16-d estimates of ANPP (Fig. 4k) resulted from the product of fPAR (Fig. 4i), PAR (Fig. 4g) and the radiation-use efficiency (εa) (Fig. 4e). All grassland classes showed again a bimodal pattern, with a clear ANPP peak in spring (maximum values in Nov) and a much smaller peak in summer (maximum values in Feb) (Fig. 4k). The difference between the spring and summer peaks is bigger in ANPP than in fPAR. The second ANPP peak was also displaced toward mid-summer, with respect to the fPAR average maximum. On average, maximum ANPP occurred in Nov and was $15.5\,kg \cdot ha^{-1} \cdot day^{-1}$ for Meso-xerophytic grasslands and Lithophytic steppes, and $18\,kg \cdot ha^{-1} \cdot day^{-1}$ for the Meso-hydrophytic grasslands (Fig. 4l). All grassland classes showed the lowest ANPP values in June (approximately $5\,kg \cdot ha^{-1} \cdot day^{-1}$) (Fig. 4l). On an annual basis, the most productive class was the Meso-hydrophytic grassland, with an average value of approximately $3800\,kg \cdot ha^{-1} \cdot yr^{-1}$. The other two units presented similar ANPP values (around $3400\,kg \cdot ha^{-1} \cdot yr^{-1}$).

The fPAR and ANPP were significantly different among the grassland classes ($F = 147$ and $F = 151$, respectively; $df = 2$, $P < 0{,}001$) in every

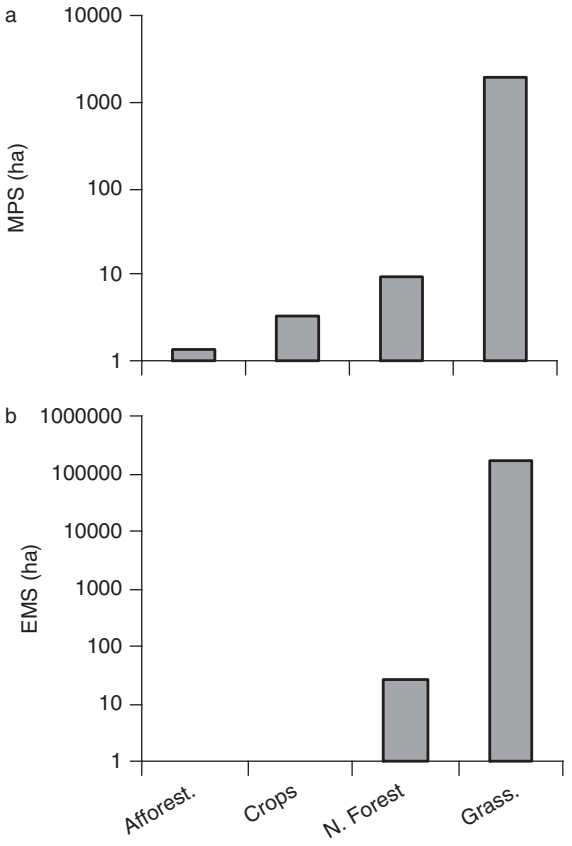

Fig. 3. Landscape metrics calculated for the study area. a) MPS: Mean Patch Size; b) EMS. Effective Mesh Size. Grass: Grasslands (includes Meso-xerophytic grasslands, Lithophytic steppes and Meso-hydrophytic grasslands). Crops (includes plowed soils, summer and winter crops); Afforest.: afforestations; N. Forest: Native Forest.

month of the average year ($F = 682$ and $F = 19\,924$, respectively; df = 11, $P < 0{,}001$), although the relative differences between them changed throughout time (Time×Unit interactions; $F = 54$ and $F = 103$, respectively; df = 22, $P < 0{,}001$). The Tukey HSD test showed significant differences ($P < 0.01$) between Meso-hydrophytic grasslands and the other two classes, except in winter months for fPAR and in autumn-winter months for ANPP values (Table 2). There were no significant differences between Meso-xerophytic grasslands and Lithophytic steppes in any month of the average year (Table 2). A multivariate test performed because of the violation of sphericity assumption for repeated measures factor (Zar 1996; Statistica, Electronic manual 2001) confirms the results of repeated measures ANOVA (Time effect: Wilk's $\lambda = 0.02$, $F = 1746$ and Wilk's $\lambda = 0.03$, $F = 10\,743$ for fPAR and ANPP, respectively, $P < 0.01$; Time×Unit interactions: Wilk's $\lambda = 0.57$, $F = 12.5$ and Wilk's $\lambda = 0.43$, $F = 19.4$ for fPAR and ANPP respectively, $P < 0.01$). Because of such different sample sizes and possible autocorrelation, we performed our analyses with all the data and randomly sub-sampled five times within the majority classes to obtain similar sample sizes. As we found the same results in all cases, we only present here the results of one of the subsamples.

The relative spatial variability of the three functional variables (fPAR, APAR and ANPP) was the same and only the ANPP data are presented in this work. The annual variation of the spatial variability of ANPP was similar among grassland units (Fig. 5). Spatial variability (among pixels) in ANPP showed a maximum in Jan and a minimum in May. Meso-hydrophytic grassland showed the lowest relative variability and Lithophytic steppes the highest, although the magnitude of the differences varied throughout the years, with maximum differences in summer (Fig. 5).

Although the grassland classes differed in the magnitude of the temporal variability of fPAR, APAR and ANPP (among years CV) the seasonality of the CV was similar among them, with an evident increase of the variation in summer months. The ANPP temporal variation was higher than the variability of fPAR and the summer peak of variation was more extended (Fig. 6).

Discussion

In this article we combined a previous phytosociological characterization of grassland communities with remote sensing techniques to provide a description of the spatial distribution of vegetation units over an extensive area of the Rio de la Plata grasslands. Our study also provided a functional characterization (e.g. ANPP seasonality) of the different plant communities of one of the most extensive areas of natural grasslands in South America. The spatial and temporal (both intra-annually and interannually) description of ANPP variability represent critical inputs to design management actions on these grasslands. Previous attempts to describe the land-cover distribution over the region lumped together different grassland types into a heterogeneous "rangelands" class (Baldi et al. 2006; Baldi & Paruelo 2008). The map generated in this study discriminates among three different grassland types based on a previous phytosociological description. The absence of vegetation maps of Uruguay precludes the comparison of our land-cover characterization with other descriptions.

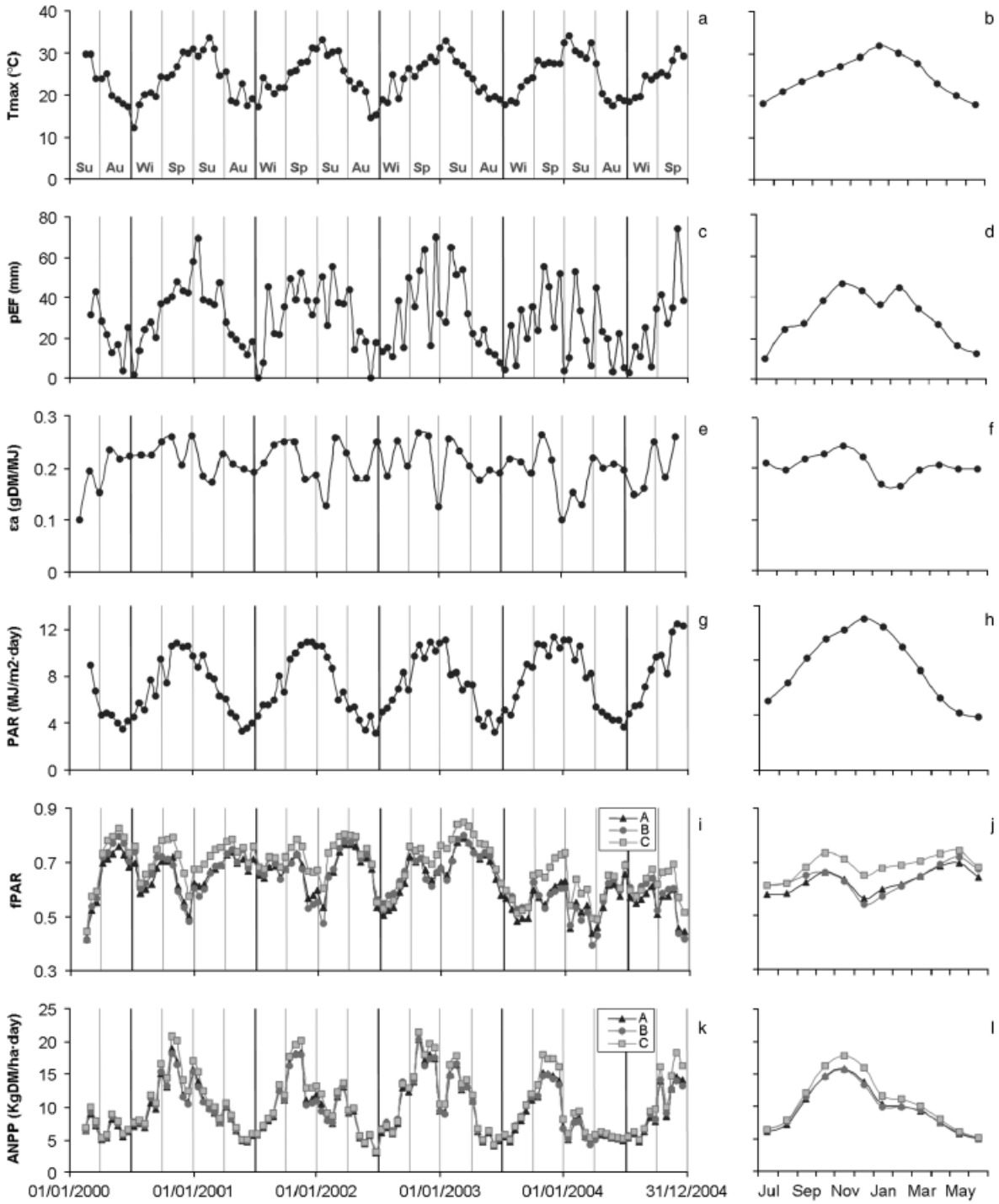

Fig. 4. Temporal variations of the analyzed variables throughout the 5 years studied (left panels) and their average annual curves (right panels). Values in left panels were integrated or averaged over a 16 days interval, except for εa (monthly intervals), while right panels are on monthly basis. Black vertical bars in the left panels show the growing seasons (July-June). (a) Tmax: maximum temperature, average for each interval; (c) pEF: effective precipitation accumulated in each interval; (e) εa: energy conversion coefficient of absorbed radiation into aboveground biomass, calculated as a function of the maximum temperature and the effective precipitation; (g) PAR: incident photosynthetically active radiation, average for each interval; (i) fPAR: fraction of photosynthetically active radiation absorbed by green vegetation, average for each grassland class; (k) ANPP: aboveground net primary production average for each grassland class, derived from PAR, fPAR and εa. (b, d, f, h, j and l); 5 years averages in monthly basis for each variable. (**a**): Meso-xerophytic grasslands; (**b**) Lithophytic steppes; (**c**) Meso-hydrophytic grasslands. Su: summer; Au: autumn; Wi: winter; Sp: Spring. See text for more details.

Table 2. Average values (in monthly basis) for the fraction of photosynthetically active radiation absorbed by green vegetation (fPAR) and aboveground net primary production (ANPP) for grassland classes. Different letters denote significant differences between grassland classes (Tukey HSD test, $P<0.01$). A = Meso-xerophytic grasslands; B = Lithophytic steppes; C = Meso-hydrophytic grasslands.

	July	August	September	October	November	December	January	February	March	April	May	June
fPAR												
A	0.57 **a**	0.57 **a**	0.62 **a**	0.66 **a**	0.63 **a**	0.57 **a**	0.60 **a**	0.62 **a**	0.64 **a**	0.67 **a**	079 **a**	0.64 **a**
B	0.61 **a**	0.62 **a**	0.65 **a,b**	0.66 **a**	0.63 **a**	0.55 **a**	0.57 **a**	0.61 **a**	0.65 **a,b**	0.69 **a,b**	0.72 **a,b**	0.68 **a**
C	0.61 **a**	0.62 **a**	0.68 **b**	0.73 **b**	0.71 **b**	0.66 **b**	0.67 **b**	0.69 **b**	0.70 **b**	0.72 **b**	0.74 **b**	0.69 **a**
ANPP ($kg \cdot DM \cdot m^{-2} \cdot d^{-1}$)												
A	6.11 **a**	7.30 **a**	11.10 **a**	14.80 **a**	15.90 **a**	13.78 **a**	10.29 **a**	10.04 **a**	9.30 **a**	7.51 **a**	5.79 **a**	4.92 **a**
B	6.47 **a**	7.71 **a**	11.44 **a,b**	14.59 **a**	15.63 **a**	13.24 **a**	9.81 **a**	9.88 **a**	9.33 **a**	7.57 **a**	5.93 **a**	5.14 **a**
C	6.42 **a**	7.67 **a**	11.92 **b**	16.13 **b**	17.68 **b**	15.88 **b**	11.49 **b**	11.04 **b**	10.05 **a**	7.94 **a**	6.10 **a**	5.20 **a**

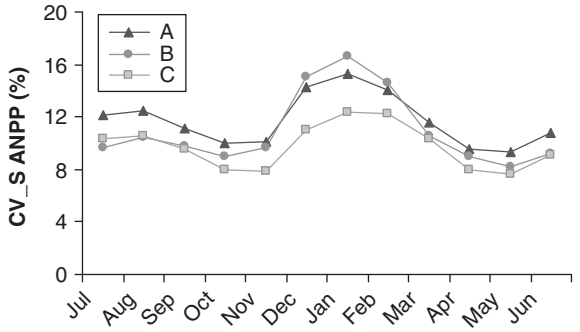

Fig. 5. Spatial (among pixels) variability in monthly Aboveground Net Primary Production (ANPP) within the three grassland units studied, expressed as the coefficient of variation (CV_S). Values are averages over the 5 years studied. (**a**) Meso-xerophytic grasslands; (**b**) Lithophytic steppes; (**c**) Meso-hydrophytic grasslands.

However, our area estimates for the different land-covers showed a good agreement with the figures of the national agricultural statistics. According to MGAP DIEA (2000) the percentage of natural grasslands in the census units included in our study area varies between 85% and 97%. For the non-grassland classes this census units shows average values of 2.8% for native forest, 1.3% for afforestations, 0.6% for winter crops and 0.2% for summer crops.

The analysis of the spatial configuration of the land-cover units showed that the fragmentation level of the grasslands was extremely low. The study area corresponds to one of the less disturbed sites of the whole Río de la Plata Grasslands biome. Saura (2002) found the EMS very suitable for comparing maps with different extents and grains. For four other areas of the Río de la Plata grasslands, Baldi et al. (2006) reported EMS values two orders of magnitude lower than those found in our analysis. The ''Flooding Pampa'' grasslands – the less fragmented grassland subregion in Baldi et al. (2006) analysis – showed an EMS average value of 41 km^2, which is much lower than found in our study (more than 1600 km^2) (Fig. 3b). According to the scale outlined by Forman (1995) and extended by Jaeger (2000) the region studied would be in incipient stages of landscape fragmentation, with big patches of undisturbed grasslands interrupted by small and isolated patches of crops and afforestations and intersected by native forest patches associated with water streams (Figs 1, 3a,b).

Despite the relative physiognomic homogeneity of the area, the spectral data provided by the MODIS/TERRA sensor allowed us to detect significant differences in carbon gains among grassland units. The dominant communities (Meso-xerophytic and Meso-hydrophytic grasslands) differed in monthly ANPP except in autumn and winter months when light and temperature constrained the production of both grassland units (Fig. 4k,l). The higher ANPP values of Meso-hydrophytic grasslands may be explained by community and edaphic attributes, such us the high values of vegetation cover of this unit and soils with greater amounts of water available for plant growth (App. 1). Lithophytic steppes seem to be a particular case of Meso-xerophytic grasslands in terms of their carbon gains. The fPAR values of Lithophytic steppes (a unit with low plant cover) were higher than expected. This unit is dominated by the spike moss *Selaginella selowii* (App. 1), a species well-adapted to xeric environments. Studies with other *Selaginella* species (*Selaginella densa*) in Canadian grasslands showed that this species may show a similar NDVI signal (and hence a similar fPAR) to those of other species of grasses and bushes (Hall-Beyer & Gwyn 1996). Additionally, *Selaginella* canopies may have different a radiation-use efficiency than the other plant functional types. Paruelo et al. (1997) showed a lower εa in xeric grassland than in humid ones. The

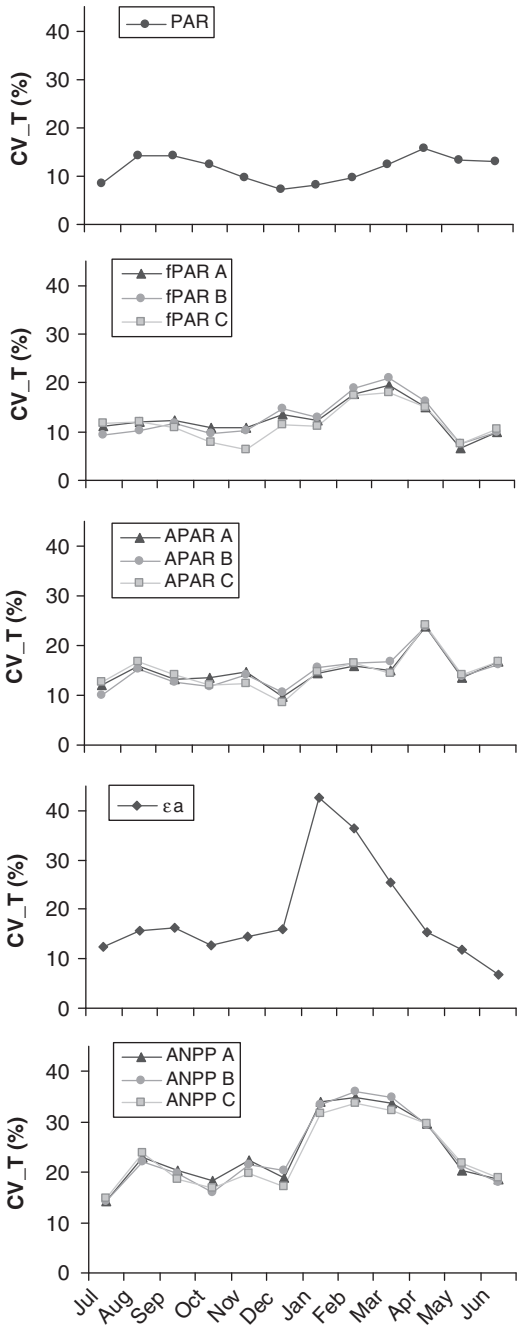

Fig. 6. Temporal (among years) variability in monthly values of the considered variables expressed as the coefficient of variation (CV_T). PAR: incident photosynthetically active radiation; fPAR: fraction of photosynthetically active radiation absorbed by green vegetation; APAR: photosynthetically active radiation absorbed by green vegetation; εa: energy conversion coefficient of absorbed radiation into aboveground biomass; ANPP: aboveground net primary production; (**a**) Meso-xerophytic grasslands; (**b**) Lithophytic steppes; (**c**) Meso-hydrophytic grasslands. fPAR, APAR and ANPP values are averages for all pixels in each unit.

model used to calculate εa was generated for mesic grasslands and is perhaps overestimating the radiation-use efficiency of the lithophytic species. Also, given the small size of the patches of this unit, we cannot rule out "contamination" of the MODIS pixel with other (more productive) units.

The bimodal seasonality of fPAR can be associated with the relative abundance of C_3 and C_4 species in the communities analysed. The spring peak would have an important contribution of C_3 (cool season) species, as found in other Uruguayan grasslands (Altesor et al. 2005) The second peak of fPAR in late summer-autumn should be related to the relative importance of C_4 grasses (Lezama et al. 2006), with a clear summer peak of photosynthetic activity (Epstein et al. 1997). An analysis based on 20 years of NOAA/AVHRR images (Pathfinder AVHRR land database, spatial resolution: 8×8 km, temporal resolution: 10 days) also identified a late summer-autumn peak of NDVI for this region of the country (Baeza et al. 2006).

Our results showed important differences between the seasonality of fPAR and ANPP. The ANPP peak of all the units was concentrated in late spring and summer when incoming radiation (PAR) is maximum (Fig. 4g-l). During summer the sharp decrease in ANPP was associated not only with a lower fPAR (probably associated with a lower leaf area caused by water stress-induced senescence) but also with a lower radiation-use efficiency. εa was low in summer because of the interaction between high temperatures and low effective precipitation (Fig. 4a,c,e). The ANPP curves generated from remotely sensed data based on Monteith's model agree with those generated from field data based on biomass harvest (Berreta & Bemhaja 1998). This study, performed on basaltic shallow soils over 14 years (1980-1994), also showed a late-spring/summer peak and a greater variability during summer months; the annual average value of forage production between the different soil types analysed in this work was $3744\,\mathrm{kg}\cdot\mathrm{ha}^{-1}\cdot\mathrm{yr}^{-1}$. The lack of superposition between the period studied by Berreta & Bemhaja (1998) and the one analysed in this work precludes a formal comparison between both datasets.

Differences in fPAR and ANPP spatial variability among vegetation units can be explained by the floristic and environmental (topographic and edaphic) differences among units. The unit showing the highest ANPP variability in space (Meso-xerophytic grasslands) (Fig. 5), was also the most variable floristically (Lezama et al. 2006). Also, soil depth, a critical control of water availability, varies between 10 and 60 cm in this unit (Lezama 2005;

Lezama et al. 2006). The soil water-holding capacity of the profile has been identified as a major determinant of ANPP in sub-humid grasslands (Sala et al. 1988). Stands of this vegetation unit may therefore experience a wide range of water availability conditions, which in turn determine fPAR and ANPP variability. The high spatial variation of summer fPAR (and ANPP) in the Lithophytic steppes should be related to rapid changes in water content of these extremely shallow soils and to the fast response of the photosynthetic activity of *Selaginella*, the dominant species of this community, to water pulses (Hall-Beyer & Gwyn 1996).

Monteith's model identifies three sources of temporal and spatial variation in ANPP: the incoming radiation, the fraction of radiation intercepted by green leaves and the efficiency of conversion of radiation into biomass. Figure 4 shows that these three variables have a different temporal variation. As a consequence, the variability of intercepted radiation (fPAR) is amplified when the radiation-use efficiency (εa) and the incident radiation (PAR) are considered in ANPP calculations. The ANPP relative variability was almost twice the variability of fPAR (Fig. 6). The εa was particularly variable in summer months due to the high variation of the effective precipitation (Fig. 4c). ANPP variability peaked during summer and early autumn (January-April) owing to the combined effect of the high variability of εa in January, February and March; and the interaction between PAR and fPAR April variations (Fig. 6).

Management implications

Our results provide valuable information for two applied issues: grazing management and grassland conservation. ANPP is the major determinant of stock density in extensive rangelands (Oesterheld et al. 1998). The availability of ANPP data is extremely scarce both in space and time. To date, ANPP for the study area has only been measured on a few scattered sites (Bemhaja 1996; Berreta & Bemhaja 1998). The estimates presented provide the basis for assessing forage availability at the paddock level. For extensive rangelands of Patagonia in Argentina, Golluscio et al. (1998) derived stock densities from remotely sensed estimates of ANPP and empirical harvest index coefficients that account for the fraction of ANPP that can be consumed by domestic herbivores (Oesterheld et al. 1992). The data presented in this work not only provides average values of ANPP to define stock carrying capacity but also identifies the range of its spatial variability: Meso-xerophytic grasslands vegetation showed an average ANPP of $3447\,kg \cdot ha^{-1} \cdot yr^{-1}$, with a range of $2750\,kg \cdot ha^{-1} \cdot yr^{-1}$. Assuming a harvest index of forage of 36.3% (Oesterheld et al. 1992; Golluscio et al. 1998) the forage available for herbivores will have a 90% chance of being between 253 and $2250\,kg \cdot ha^{-1} \cdot yr^{-1}$. Given an average consumption of a sheep of $365\,kg \cdot ha^{-1} \cdot yr^{-1}$ the estimated stocking density will vary in space between 0.7 and $6.2\,sheep\,ha^{-1}$. Such spatial variability illustrates the problem that arises when point data are extrapolated to larger areas and the advantages of spatially exhaustive methods to assess carrying capacity (Golluscio et al. 1998), and the risk of a general definition of stocking densities over large areas.

Just as important as characterizing ANPP spatial variability is describing the seasonal and interannual changes in the rate of biomass accumulation. Monthly average values of ANPP and estimates of their temporal variability are critical pieces of information to derive forage budgets and to quantify risk and efficiency in livestock production (Grigera et al. 2007). Our results, for example, highlighted a contrast in interannual variability between summer and late spring. Summer not only had a lower ANPP (Fig. 4k, l) but also it showed a high interannual variability (Fig. 6). These two pieces of information on forage availability provide a useful tool to manage livestock production systems.

As ANPP estimates at the pixel scale are associated with a floristic characterization, it is possible to derive estimates of forage quality based on herbivore preference for the dominant species of the community. The inertia or temporal autocorrelation of the ANPP data (Wiegand et al. 2004) allows us to define a range of expected values of production at least 1 month ahead. This information, and algorithms capable of modelling the influence of water availability scenarios, are the basis of devising "warning systems" for forage availability.

An improved grazing management scheme will contribute in itself to grassland conservation. A definition of carrying capacity based on ANPP data may help reduce overgrazing and grassland degradation. However, our results may make additional contributions to this goal. First, we identified the spatial distribution and location of targeted entities of conservation plans: plant communities. By identifying the connectivity between patches of different classes our map provided elements to define actions to protect communities and species (i.e. size and distribution of protected areas). Second, the functional analysis presented is the basis to devise monitoring programs able to detect trends in ecosystems functioning associated with either

management-forcing variables or global change drivers (climate and atmospheric composition).

Finally, our work provides valuable information to evaluate the role of grassland heterogeneity on ecosystem health and its impact on biodiversity maintenance. Several authors pointed out that high levels of spatial and temporal vegetation variability promote the conservation of species of higher trophic levels (Benton et al. 2003; Fuhlendorf et al. 2006; Briske et al. 2008). Here we provided methods and information to evaluate the spatial and temporal heterogeneity of grasslands, which provide the basis for habitat quality evaluation to test hypotheses about the impact of heterogeneity on biodiversity and to define better conservation and livestock production practices.

Acknowledgements. Research was partly funded by FONTAGRO (IICA/BID FTG/RF 0103RG), FPTA 175 – INIA, SENSOR – TTC 003874–2 (Uruguay and Argentine partners) and by a grant from the Inter-American Institute for Global Change Research (IAI, CRN II 2031), which is supported by the US National Science Foundation (Grant GEO-0452325). We thank the members of the Laboratorio de Análisis Regional y Teledetección, IFEVA, FAUBA for their help in the processing of IVN-MODIS images and Germán Baldi for providing special help for the landscape analysis. We thank Aaron Moody and two anonymous reviewers for their support and comments.

References

Altamirano, A., Da Silva, H., Durán, A., Echeverría, A., Panario, D. & Puentes, R. 1976. *Carta de reconocimiento de suelos del Uruguay. Tomo III, Clasificación de Suelos*. Dirección de Suelos y Fertilizantes. Ministerio de Agricultura y Pesca, Montevideo, UY.

Altesor, A., Oesterheld, M., Leoni, E., Lezama, F. & Rodríguez, C. 2005. Effect of grazing on community structure and productivity of a Uruguayan grassland. *Plant Ecology* 179: 83–91.

Anon. (Dirección Nacional de Meteorología) 2005. Estadísticas climatológicas 1961–1990. Available at http://www.meteorologia.com.uy/estadistica_climat.htm (accessed 1 September 2008).

Anon (Ministerio de Ganadería Agricultura y Pesca.). Dirección de Estadísticas Agropecuarias (MGAP, DIEA). Censo general Agropecuario 2000. Available at http://www.mgap.gub.uy (accessed 1 September 2008).

Baeza, S., Paruelo, J.M. & Altesor, A. 2006. Caracterización funcional de la vegetación de Uruguay mediante el uso de sensores remotos. *Interciencia* 31: 382–388.

Baldi, G. & Paruelo, J.M. 2008. Land use and land cover dynamics in South American temperate grasslands. *Ecology and Society*. 13 (2): 6. [online] URL: http://www.ecologyandsociety.org/vol13/iss2/art6/

Baldi, G., Guerschman, J.P. & Paruelo, J.M. 2006. Characterizing fragmentation in temperate South America grasslands. *Agricultural Ecosystem and Environment* 116: 197–208.

Bemhaja, M. 1996. Producción de pasturas en Basalto. *INIA Serie Técnica* 80: 231–240.

Benton, T.G., Vickery, J.A. & Wilson, J.D. 2003. Farmland biodiversity: is habitat heterogeneity the key? *Trends in Ecology and Evolution* 18: 182–188.

Berreta, E.J. & Bemhaja, M. 1998. Producción estacional de comunidades naturales sobre suelos de Basalto en la Unidad Queguay Chico. *INIA, Serie Técnica* 102: 11–20.

Briske, D.D., Derner, J.D., Brown, J.R., Fuhlendorf, S.D., Teague, W.R., Havstad, K.M., Gillen, R.L., Ash, A.J. & Willms, W.D. 2008. Rotational Grazing on Rangelands: reconciliation of perception and experimental evidence. *Rangeland Ecology and Management* 61: 3–18.

Brown de Colstoun, E.C., Story, M.H., Thompson, C., Commisso, K., Timothy, G., Smith, T.C. & Irons, J.R. 2003. National park vegetation mapping using multitemporal Landsat 7 data and a decision tree classifier. *Remote Sensing of Environment* 85: 316–327.

Chavez, P.S. 1996. Image-based atmospheric corrections. Revisited and improved. *Photogrammetric Engineering and Remote Sensing* 62: 1025–1036.

Chuvieco, E. 2002. *Teledetección ambiental. La observación de la Tierra desde el espacio*. Editorial Ariel, Barcelona, ES.

Congalton, R. 1991. A review of assessing the accuracy of classifications of remotely sensed data. *Remote Sensing of Environment* 37: 35–46.

Di Bella, C.M., Paruelo, J.M., Becerra, J.E., Bacour, C. & Baret, F. 2004. Effect of senescent leaves on NDVI-based estimates of fAPAR: experimental and modeling evidences. *International Journal of Remote Sensing* 25: 5415–5427.

Epstein, H.E., Lauenroth, W.K., Burke, I.C. & Coffin, D.P. 1997. Productivity patterns of C_3 and C_4 functional types in the U.S. Great Plains. *Ecology* 82: 722–731.

Forman, R.T.T. 1995. *Land mosaics. The ecology of landscapes and regions*. Cambridge University Press, Cambridge, UK.

Fuhlendorf, S.D., Harrell, W.C., Engle, D.M., Hamilton, R.G., Davis, C.A. & Leslie, D.M. Jr. 2006. Should heterogeneity be the basis for conservation? Grassland bird response to fire and grazing. *Ecological Applications* 16: 1706–1716.

Golluscio, R.A., Deregibus, V.A. & Paruelo, J.M. 1998. Sustainability and range management in the Patagonian steppes. *Ecología Austral* 8: 265–284.

Grigera, G., Oesterheld, M. & Pacín, F. 2007. Monitoring forage production for farmers' decision making. *Agricultural Systems* 94: 637–648.

Guershman, J.P., Paruelo, J.M., Di Bella, C., Giallorenzi, M.C. & Pacin, F. 2003. Land cover classification in the Argentine Pampas using multi-temporal Landsat TM data. *International Journal of Remote Sensing* 24: 3381–3402.

Hall-Beyer, M. & Gwyn, Q.H.J. 1996. *Selaginella densa* reflectance: relevance to rangeland remote sensing. *Journal of Range Management* 49: 470–473.

Jackson, R.D., Hatfield, J.L., Reginato, R.J., Idso, S.B. & Pinter, P.J. Jr. 1983. Estimation of daily evapotranspiration from one time-of-day measurements. *Agricultural Water Management* 7: 351–362.

Jaeger, J.A.G. 2000. Landscape division, splitting index, and effective mesh size: new measures of landscape fragmentation. *Landscape Ecology* 15: 115–130.

Jobbágy, E.G., Vasallo, M., Farley, K.A., Piñeiro, G., Garbulsky, M.F., Nosetto, M.D., Jackson, R.B. & Paruelo, J.M. 2006. Forestación en pastizales: hacia una visión integral de sus oportunidades y costos ecológicos. *Agrociencias* 10: 109–124.

Lavorel, S., McIntyre, S., Landsberg, J. & Forbes, T.D.A. 1997. Plant functional classifications: from general groups to specific groups based on response to disturbance. *Trends in Ecology & Evolution* 12: 474–478.

Lezama, F. 2005. Las comunidades herbáceas de un área de pastizales naturales de la Región Basáltica, Uruguay. Tesis PEDECIBA, Biología, Facultad de Ciencias, Montevideo, UY.

Lezama, F., Altesor, A., León, R.J., Paruelo, J.M. 2006. Heterogeneidad de la vegetación en pastizales naturales de la región basáltica de Uruguay. *Ecología Austral* 16: 167–182.

Lillesand, T. & Kiefer, R. 1994. *Remote sensing and image interpretation*. 3rd ed. John Wiley & Sons, New York, NY, US.

McNaughton, S.J., Oesterheld, M., Frank, D.A. & Williams, J.K. 1989. Ecosystem-level patterns of primary productivity and herbivory in terrestrial habitats. *Nature* 341: 142–144.

Monteith, J.L. 1972. Solar radiation and productivity in tropical ecosystems. *Journal of Applied Ecology* 9: 747–766.

Oesterheld, M., Sala, O.E. & Naughton, S.J. 1992. Effect of animal husbandry on herbivore-carrying capacity at a regional scale. *Nature* 356: 234–236.

Oesterheld, M., DiBella, C.M. & Kerdiles, H. 1998. Relation between NOAA AVHRR satellite data and stocking rate of rangelands. *Ecology Application* 8: 207–212.

Panario, D. 1988. *Geomorfología del Uruguay*. Publicación de la Facultad de Humanidades y Ciencias, Universidad de la República, Montevideo, UY.

Paruelo, J.M., Epstein, H.E., Lauenroth, W.K. & Burke, I.C. 1997. ANPP estimates from NDVI for the central grasslands region of the U.S. *Ecology* 78: 953–958.

Paruelo, J.M., Jobbajy, E. & Sala, O.E. 2001. Current distribution of ecosystem functional types in temperate South America. *Ecosystem* 4: 683–698.

Paruelo, J.M., Guershman, J.P., Baldi, G. & Di Bella, C. 2004a. La estimación de la superficie agrícola. Antecedentes y una propuesta metodológica. *Interciencia* 29: 421–427.

Paruelo, J.M., Guershman, J.P., Piñeiro, G., Jobbágy, E.G., Verón, S.R., Baldi, G. & Baeza, S. 2006. Cambios en el uso de la tierra en Argentina y Uruguay: marcos conceptuales para su análisis. *Agrociencia* 10: 47–61.

Paruelo, J.M., Jobbágy, E.G., Oesterheld, M., Golluscio, R.A. & Aguiar, M.R. 2007. The grasslands and steppes of Patagonia and the Rio de la Plata plains. In: Veblen, T., Young, K. & Orme, A. (eds.) *The physical geography of South America*. pp. 232–248. Oxford University Press, Oxford, UK.

Piñeiro, G., Paruelo, J.M. & Oesterheld, M. 2004. Estimación regional de la productividad del campo natural mediante sensores remotos. In: Proc. XX Reunión del grupo Campos-Cono Sur, p. 243–244. Facultad de Agronomia, UDELAR, Montevideo UY.

Piñeiro, G., Oesterheld, M. & Paruelo, J.M. 2006a. Seasonal variation in aboveground production and radiation-use efficiency of temperate rangelands estimated through remote sensing. *Ecosystems* 9: 357–373.

Piñeiro, G., Paruelo, J.M. & Oesterheld, M. 2006b. Potential long-term impacts of livestock introduction on carbon and nitrogen cycling in grasslands of Southern South America. *Global Change Biology* 12: 1267–1284.

Prince, S.D. 1991. Satellite remote sensing of primary production: comparison of results for Sahelian grasslands 1981–1988. *International Journal of Remote Sensing* 12: 1301–1311.

Rawls, W. 1983. Estimating soil bulk density from particle size analysis and organic matter content. *Soil Science* 135: 123–125.

Riitters, K.H., O'Neill, R.V., Hunsaker, C.T., Wickham, J.D., Yankee, D.H., Timmins, S.P., Jones, K.B. & Jackson, B.L. 1995. A factor analysis of landscape pattern and structure metrics. *Landscape Ecology* 10: 23–39.

Rodríguez, C., Leoni, E., Lezama, F. & Altesor, A. 2003. Temporal trends in species composition and plant traits in natural grasslands of Uruguay. *Journal of Vegetation Science* 14: 433–440.

Roy, D.P., Borak, J.S., Devadiga, S., Wolfe, R.E., Zheng, M. & Descloitres, J. 2002. The MODIS Land product quality assessment approach. *Remote Sensing of Environment* 83: 62–76.

Ruimy, A., Saugier, B. & Dedieu, G. 1994. Methodology for the estimation of terrestrial net primary production from remotely sensed data. *Journal of Geophysical Research* 99: 5263–5283.

Sala, O.E. & Austin, A.T. 2000. Methods of estimating aboveground net primary productivity. In: Sala, O., Jackson, R., Mooney, H. & Howarth, R. (eds.) *Methods in ecosystem science*. pp. 31–43. Springer, New York, NY, US.

Sala, O.E., Parton, W.J., Joyce, L.A. & Lauenroth, W.K. 1988. Primary production of the central grassland region of the United States: spatial pattern and major controls. *Ecology* 69: 40–45.

Saura, S. 2002. Effects of minimum mapping unit on land cover data spatial configuration and composition. *International Journal of Remote Sensing* 23: 4853–4880.

Soriano, A. 1991. Río de la Plata Grasslands. In: Coupland, R.T. (ed.) *Natural Grasslands. Introduction and Western Hemisphere*. pp. 367–407. Elsevier, Amsterdam, NL.

Wiegand, T., Snyman, H.A., Kellner, K. & Paruelo, J.M. 2004. Do grasslands have a memory: modelling phytomass production of a semiarid South African grassland. *Ecosystems* 7: 243–258.

Zar, J.H. 1996. *Biostatistical analysis*. 3rd ed. Prentice Hall, NJ, US.

Zuloaga, F.O., Nicora, E.G., Rúgolo de Agrasar, Z.E., Morrone, O., Pensiero, J. & Cialdella, A.M. 1994. *Catálogo de la Familia Poaceae en la Argentina*. Monographs in Systematic Botany from the Missouri Botanical Garden. 47: 1–178.

Zuloaga, F.O. & Morrone, O. 1996a. *Catálogo de plantas Vasculares de la República Argentina I*. Monographs in Systematic Botany from the Missouri Botanical Garden. 60: 1–1323.

Zuloaga, F.O. & Morrone, O. 1996b. *Catálogo de plantas Vasculares de la República Argentina II*. Monographs in Systematic Botany from the Missouri Botanical Garden. 74: 1–1269.

App. 1

Macrotopography, physiognomy and list of indicator species of the vegetation units studied. Vegetation cover: these are given as modal values with minimum and maximum values in parenthesis Table A1.

Received 4 November 2008;
Accepted 16 July 2009.
Co-ordinating Editor: A. Moody

Table A1. The plant functional type corresponding to each species is presented in parenthesis: CS-g = cool-season grass; WS-g = warm-season grass; A-g = annual grass; F = forb; Sh = shrub; J-C = Cyperaceae or Juncaceae; L = legume.

Vegetation Unit	Microtopography	Physiognomy	Indicator species
Meso-xerophytic grasslands	Shallow soils on steep and gentle slopes and convex interfluves of hills	Two strata mosaic: low (5–10 cm) with grasses and forbs, high (30 cm) dominated by erect grasses and the sub shrub *Baccharis coridifolia* Soil cover: 95 (40, 95)	*Piptochaetium montevidense (CS-g)* *Richardia humistrata (F)* *Baccharis coridifolia (Sh)* *Botriochloa laguroides (WS-g)* *Wahlenbergia linarioides (F)* *Schizachyrium spicatum (WS-g)* *Ayenia mansfeldiana (F)* *Eragrostis neesii (WS-g)* *Aristida venustula (WS-g)* *Oenothera* sp. (F)
Lithophytic steppes	Flat erosion surfaces at high and middle topographical positions	One open herbaceous stratum of 5–10 cm height, basically a mosaic of patches dominated by *Selaginella sellowii* (a prostrated spike moss) interspersed among rocky outcrops Soil cover: 50 (15, 80)	*Hordeum pusillum (A-g)* *Selaginella sellowii* *Portulaca papulosa (F)* *Euphorbia pampeana (F)* *Bulbostylis sp. (J-C)* *Richardia stellaris (F)* *Tripogon spicatus* (WS-g)
Meso-hydrophytic grasslands	Deep soils of gentle low slopes, valleys and plains	Two strata: one stratum of prostrate grasses and graminoids (< 5 cm) and one stratum of erect grasses (30 cm) Soil cover:100 (75, 100)	*Paspalum dilatatum (WS-g)* *Scutellaria racemosa (F)* *Coelorhachis selloana (WS-g)* *Axonopus affinis (WS-g)* *Panicum hians (WS-g)* *Mecardonia montevidensis (F)* *Piptochaetium stipoides(CS-g)* *Stipa charruana (CS-g)* *Rhynchospora luzuliformis (J-C)* *Aristida uruguayensis(WS-g)*